Basics and Advances of Quantitative PET Imaging

13

Magdy M. Khalil

Contents

13.1 **Introduction** 304

13.2 **PET Quantitation** 304
13.2.1 Spectrum of PET Quantitation 305
13.2.2 Static PET Imaging 305
13.2.3 Dynamic PET Imaging 306
13.2.4 Static Versus Dynamic PET 309

13.3 **Standardized Uptake Value (SUV)** 310
13.3.1 Drawbacks of SUV 311
13.3.2 SUV Variants 311

13.4 **Total Disease Burden** 312

13.5 **Factors Affecting Quantitative Measurements** 313
13.5.1 Biological Factors 314
13.5.2 Blood Glucose Level 314

13.6 **Response to Therapy** 315

13.7 **Tumor Texture Analysis** 317

Conclusion 318

References 318

Abstract

Positron emission tomography (PET) has been enjoying outstanding quantitative features since its inception in diagnostic clinical imaging. These capabilities have served the evolution and diagnostic performance of PET in many circumstances including research and development as well as clinical routines. However, this has been made with extensive efforts exerted on technical, physical, and instrumental levels. Quantitative PET can be very simple but also sometimes need to be very complicated and cumbersome. This depends heavily on the purpose of the imaging task. Static and dynamic PET are the two different modes of data acquisition from which the relevant type of information is extracted and physiologically interpreted. The most commonly used form of data quantitation in PET is the standardized uptake value (SUV) that may take several forms. This later quantitative index, despite being simple to calculate showing effectiveness in a number of malignancies, is prone to many technical and biological errors if not properly adjusted. All of the above have been reviewed in this chapter along with other new emerging volumetric and disease burden quantitative metrics.

M.M. Khalil, PhD
Medical Biophysics, Department of Physics,
Faculty of Science, Helwan University, Cairo, Egypt
e-mail: magdy_khalil@hotmail.com

M.M. Khalil (ed.), *Basic Science of PET Imaging*, DOI 10.1007/978-3-319-40070-9_13

13.1 Introduction

Positron emission tomography (PET) is a well-established and standard diagnostic imaging modality in clinical practice. The major role has become very evident in oncology with useful diagnostic capabilities in other areas of medicine that include neurology, cardiology, infection, and inflammation. In 2007, the Society of Nuclear Medicine and Molecular Imaging defined molecular imaging as "the visualization, characterization, and measurement of biological processes at the molecular and cellular levels in humans and other living systems." PET imaging using F18-flurodeoxyglucose has a high sensitivity in detecting glucose avid malignant tumors. This phenomenon was originally initiated by Warburg in 1930s [1, 2]. In contrast to normal differentiated cells, which rely primarily on mitochondrial oxidative phosphorylation to generate the energy needed for cellular processes, most cancer cells instead rely on the non-efficient aerobic glycolysis [3]. During this process, glucose uptake is enhanced by upregulation of glucose transporters (GLUT), increased levels of hexokinase, and decreased levels of glucose-6-phosphatase [4].

PET imaging has a unique molecular sensitivity as it can use very small amount of radiotracer in the range of nano- to picomolar concentration in detection of functional disorders within human body without disturbing the normal biochemistry or pharmacokinetics of the target tissue. This detection capability is a central point in characterizing PET systems over other imaging modalities. Therefore, there is a continuous interest to improve overall system performance in terms of spatial resolution, sensitivity, count rate performance, timing, and energy resolution in connection to developing new advanced correction and reconstruction algorithms. These developments have several consequences on image quality and quantitative accuracy of PET examinations.

PET is a multidisciplinary functional and molecular diagnostic tool with enhanced morphological features when combined with structural imaging modalities such as x-ray computed tomography (CT) and magnetic resonance imaging (MRI). These relatively new hybrid imaging modalities bring to reading physicians a significant amount of information not only on qualitative (i.e., visual assessment) level but also have a substantial influence on quantitative and semi-quantitative measurements.

PET/CT has gained a wide acceptance among nuclear medicine practitioners and scientific community owing to the fact of improved diagnostic performance and guiding clinicians toward better patient management. Applications of PET/CT in oncology are of particular importance and include initial diagnosis, staging, restaging, recurrence detection, monitoring response to treatment, as well as patient stratification and prognostication.

The multimodality hybrid imaging approach has proved its clinical significance in more than one aspect. Together with time reduction, speed of diagnosis, incremental diagnostic information, and advising on proper treatment strategy, hybrid imaging will play a very essential tool in future of modern medicine or more specifically on practice of what is recently called personalized or precision medicine [5].

13.2 PET Quantitation

Despite the fact that visual interpretation is the conventional method of reading PET imaging data, it has been shown that quantitative analysis allows an objective complement in supporting diagnostic and decision-making process [6]. The term "quantitation" has several interpretations among PET imaging practitioners, and range from simple detection and determination of tracer concentrations may be in units of kBq/ml, μCi/ml to more sophisticated mathematical algorithms that indicate rate of tracer transportation or exchange among different biochemical species or tissue space [7, 8]. What determines the level of complexity of quantitation is the target biological question and objective of the PET study which might be a development of new PET radiopharmaceutical and examining tracer biodistribution, diagnostic workup and staging, response to treatment, or investigating efficacy of new therapeutic drugs as can be seen and performed in clinical trials [9].

We may classify quantitative approaches in PET imaging into three major types, namely, qual-

itative methods using visual assessment, semiquantitative methods using standardized uptake value (SUV) and its variants, and absolute measurements of tracer pharmacokinetics using kinetic modeling analysis. Two major types of data acquisition are available in PET that permits one to perform the required type of image quantitation; these are static and dynamic imaging. Static images are normally acquired when the tracer is injected and an adequate time is given for tracer clearance from plasma and accumulation into the tissue to improve target-to-nontarget ratio. However, dynamic imaging as the name implies does capture the metabolic information on a real time fashion enabling one to derive valuable physiologic quantitative parameters as will be discussed later.

13.2.1 Spectrum of PET Quantitation

Interpretations of FDG PET scan depend in large part on well understanding of the normal physiologic uptake and associated normal variants in addition to imaging pitfalls. This supports the reading physician to come up with clear idea about abnormal finding whether it is a true pathology or normal physiologic uptake. However, this process is subject to a significant inter-reader variability and less quantitative base.

A reliable and reproducible measure of tracer uptake within different pathologic lesions of cancer as well as other disease pathologies has several advantages and benefits. Elimination of inter-reader variability is the first outcome of these quantitative or semiquantitative metrics in PET image interpretation. Another aim of having this type of measurement is the possibility of comparison among different patient studies typically in monitoring and assessment of response to treatment. A robust, reliable, and distinctive cutoff value of the response is ideally desirable to support the decision-making process for a given treatment line [10]. It would also be very helpful in predicting the success of a chosen therapy over others especially at early cycles of selected therapeutic regimen. On the other side, such a metric could provide a more insight into the spectrum and biological heterogeneity of a specific disease and particularly in inter-patient comparisons. The development of novel targeted tracers imposes the use of a suitable or optimal quantitative method as conventional quantitative metrics may not always be adapted for extracting relevant information [11].

A standardized imaging protocol and quantification strategy would also permit an easy comparison among different PET clinics to build up a knowledge base with minimal observer variability and methodological preferences. This can take place if the method is well defined and sources of technical errors and imaging pitfalls are recognized and eliminated [12]. Therefore, standardized quantification facilitates multicenter trials, allows comparison among different PET clinics, and supports the way toward personalized therapy [13]. These properties are not limited only to oncology applications, but there is a growing interest to use PET quantitative indices in infection and inflammatory disorders in addition to the existing interest in neurology and cardiology [14].

13.2.2 Static PET Imaging

After the advent of PET/CT more than a decade ago, there was a paradigm shift in the practice of PET imaging in terms of its impact on management of cancer patients and hence on clinical oncology [15]. The standard PET/CT imaging protocol in oncology is normally a whole-body scanning procedure that extends from skull base to mid-thigh. Most imaging procedures start around 60 min post-activity administration, and patient is allowed to relax in a room of moderate light intensity after intravenous injection. Patients should fast for 4–6 h to minimize the effect of endogenous glucose and avoid its competition with the injected glucose analogue F18-FDG during the uptake period. The CT examination often starts before the multiple bed positions used for acquiring the PET. The former is launched by acquiring a scout view that is then used by the user to delimit the whole-body segment required for CT and PET scan length. Contrast-enhanced CT might be performed after PET acquisition to avoid the possibility of image

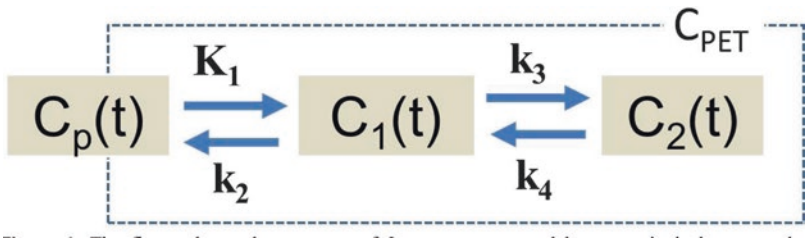

Fig. 13.1 The figure shows the structure of three-compartment model to quantitatively assess the transportation rate constants related to FDG metabolism, where C_p, C_1, and C_2 are the compartments for plasma, free, and metabolized tracer, respectively. C_{PET} represents what the scanner measures in a voxel or in a region of interest (ROI). The rate constants K_1–k_4 regulate the tracer transportation through the different compartments which could be a transfer from chemical species to another or from physical space to another physical space. Note that K_1 is the perfusion and has units in ml/g/min, while k_2–k_4 have units in 1/min. The measured PET signal is contaminated by a fraction of tracer concentration in plasma, and this question is addressed by including a portion of the input function in the kinetic model equation (Adapted from Bentourkia [7])

artifacts due to contrast deposition in some regions of the body [16, 17].

Image reconstruction using iterative techniques (reviewed in Chap. 11) has become widely available due to many reasons including improved noise characteristics, contrast and spatial resolution, and ultimately quantitative accuracy and image quality. As mentioned, the PET data are acquired using sequential multiple bed scanning approach applying 2–5 min for each bed position. This heavily depends on the adopted imaging protocol that is affected by PET system performance and the employed F18-FDG dosing and uptake period. The most common form of image quantitation is the use of the standardized uptake value (SUV) as an adjunct in image interpretation.

13.2.3 Dynamic PET Imaging

Apart from static whole-body PET examinations, dynamic imaging reveals several important physiologic and metabolic information of tracer pharmacokinetic behavior in tissues and has been extensively used in a number of potential applications in neurology, cardiology, and oncology [11, 18, 19]. It can be acquired with predetermined number of frames and the duration of each or group of frame(s). List mode data acquisition, however, is one tool that can be used to record events based on their specific attributes such as time and energy but at the cost of high storage demands. This type of acquisition provides opportunity to reframe acquired data at any arbitrary time frame.

Dynamic PET provides the possibility of absolute data quantitation based on compartmental or non-compartmental methods and quantitative estimation of tracer kinetics relying on region or voxel of interest analysis. The approach of using individual voxel as separate input to the pharmacokinetic model is termed parametric data analysis and provides more insights into spatial distribution of the radiotracer kinetics. However, it suffers from image noise and requires more computational resources [20]. Kinetic modeling does assist in deriving biologically relevant parameters, such as vascular transport and cellular metabolism, and asks for determination of the blood activity concentration of the native tracer over time as an input function to the model [21]. A compartment model of glucose metabolism is illustrated in Fig. 13.1. Mathematical bases of kinetic modeling are reviewed in Chap. 14.

In PET cardiac imaging, determination of myocardial blood flow and flow reserve can be measured using dynamic scanning of the heart region using some radiotracers such as O15-water, ammonia (N13), Rubidium-82 (Rb82), and other tracers that exhibit blood flow characteristics. Quantitation of myocardial blood flow using dynamic PET is reviewed in Chap. 19.

In neurology, dynamic PET has been a very useful tool in determination of important physiologic measures that reflect tracer receptor density, distribution volume, drug occupancy, and

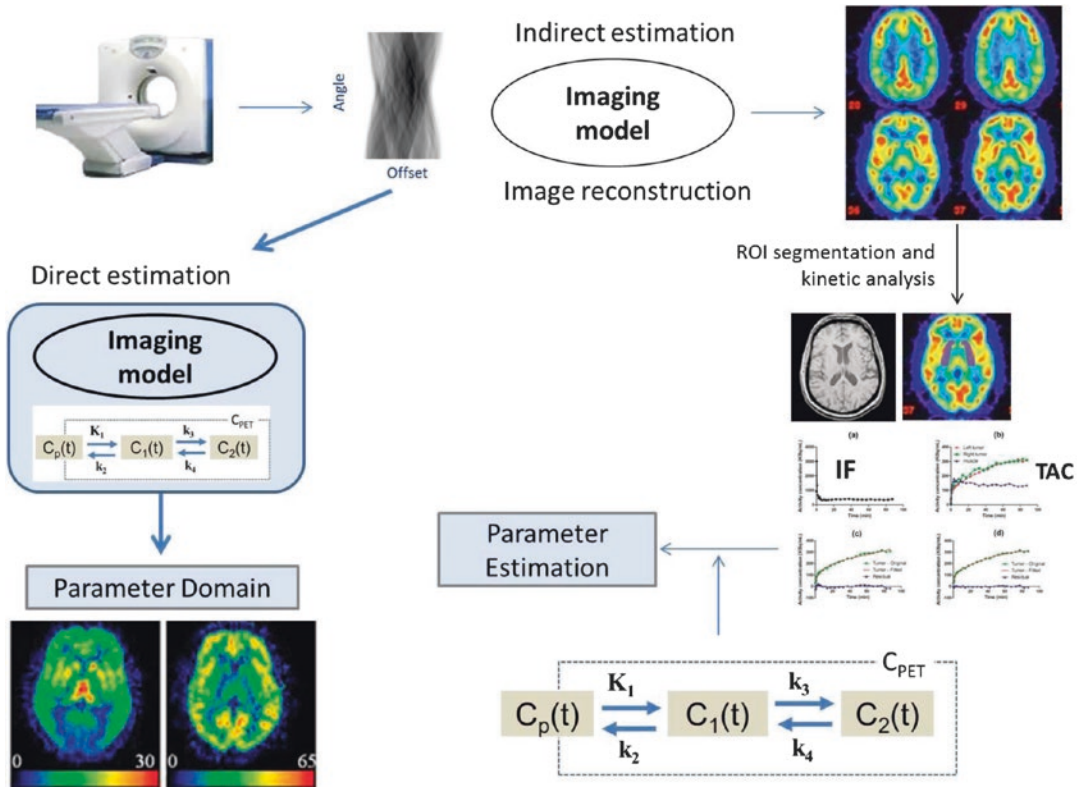

Fig. 13.2 Dynamic PET is used to determine valuable metabolic and functional parameters. The standard protocol relies on delineating regions of interest (ROIs) on a summed PET image reconstructed using the system model or a co-registered anatomical image. Time-activity curves (TACs) from the ROIs with collected information about tracer concentration in plasma (i.e., input unction, IF) are used in the kinetic model to derive the physiologic tracer parameters. The other way around is to calculate rate parameters directly from sinogram data with less noisy estimates (Modified from Muzi et al. [21])

very instrumental tool in drug development [22]. In oncology, pharmacokinetic modeling provides valuable opportunities for measurements of receptor density of potential therapeutic targeting, determination of tumor blood flow, as well as measuring the efficacy of anticancer drugs [23].

Dynamic PET imaging-derived kinetic parameters, particularly transport (flow) and overall metabolic rate, have provided imaging endpoints for clinical trials at single-center institutions for years. However, dynamic imaging poses many challenges for multicenter clinical trial implementations from cross-center calibration to the inadequacy of a common informatics infrastructure [21]. Figure 13.2 illustrates the imaging workflow of static and dynamic PET image acquisition and data analysis. One recent study revealed that the influx rate constant K_i determined by Patlak graphical method in simulation and patient data has better contrast-to-noise ratio (a measure related to more reliable tumor detection), and this has remarkable advantage in lesions of high uptake surrounded by elevated but constant background levels such as liver lesions. Meanwhile, SUV performance was relatively poor [24]. Another study have used different methods for quantification of tumor activity (in a group of 40 patients with colon cancer metastatic to the liver) including SUV, Patlak graphical analysis, simplified kinetic model, and metabolic rate of glycolysis (MRGlu). Overall, Patlak was the best predictor of outcome and best discriminator between normal tissue and tumor results [25].

Several attempts have been devised to correlate the kinetically derived tracer influx rate constant K_i to SUV measurements by either making

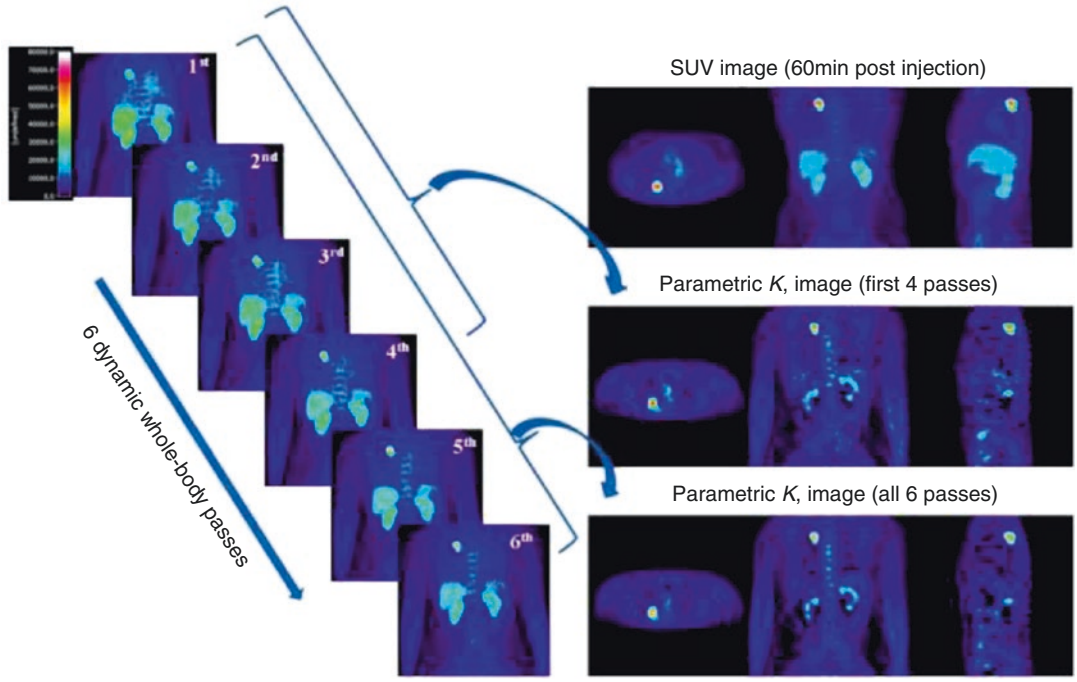

Fig. 13.3 Patlak analysis using six sequential whole-body PET scans. The last six whole-body dynamic frames are shown on the left side. On the right side: the SUV image, the K_i parametric image derived from all six last frames, and the K_i image after omitting the last two frames (Reprinted with permission from Karakatsanis et al. [24] and thanks to Dr Nicolas Karakatsanis for providing some clarification on the figure)

strong assumptions that could be violated in practice or still function of the imaging time point [26, 27]. The measuring time point is very crucial in estimating the metabolic activity, and wide variation could be found in different malignancies and in individual patients; therefore, quantitative image interpretation should be cautiously undertaken. Benign and inflammatory lesion uptake time could be within 30–60 min, while malignant tissues exhibit wide variation across patients that may reach plateau after 4 h [28]. Thus, recommendations are often taken to be within 50–70 min and not much longer to minimize the effect of tracer decay [29–31].

For example, dynamic F18-FDG PET imaging was found to accurately differentiate malignant from benign pulmonary lesions in patients with suspected malignant pulmonary lesions. SUV and visual assessment were outperformed by dynamic imaging data analysis in differentiating benign and malignant lesions [32]. However, whole-body dynamic PET imaging is not feasible at the moment due to limited axial field of view of most commercial PET scanners.

In a recent work, researchers proposed a new solution where dynamic whole-body imaging can be made feasible using the current PET/CT generation systems [24, 33]. It consists of a 6 min initial scan over the heart to extract the input function through image-based method to get rid of the cumbersome work associated with arterial catheterization. This action is followed by six passes of dynamic whole-body scanning including subsequent passes over the heart. Standard Patlak linear graphical analysis modeling is then applied at the voxel level to derive parametric images of K_i that reflects net tracer uptake [33]. The method looks interesting and combines between feasibility and advantages of dynamic quantitative features, but further work is needed to explore its potential in routine practice of patient diagnosis and therapeutic applications.

In Fig. 13.3 and in the SUV image, the patient was scanned with arms in the up position,

according to the conventional whole-body PET protocol recommendations to limit the attenuation from the arms. However, for the whole-body dynamic protocol, the patient had to be scanned for approximately 45 min with arms down due to the lengthy period of the scan. It was observed that the additional attenuation that may be caused because of that position does not affect the quality of the data [24].

13.2.4 Static Versus Dynamic PET

As described, the net FDG influx rate constant K_i (mL blood/mL tissue/min) is a valuable quantitative measure that reflects the hexokinase and enzymatic capacity of the tumor cells. This measure was found to correlate with SUV measurements taking two conditions into account as outlined by Kotasidis et al. [26]:

1. The time integral of plasma FDG concentration is proportional to the injected dose divided by body weight (BW), lean body mass (LBM), or body surface area (BSA) as defined in the SUV formula. However, this assumption is not always valid due to, for example, treatment intervention that might interfere or influence dynamics of FDG in plasma, and a simple correlation with injected dose and BW, BSA, or LBM would not be effective.
2. Non-phosphorylated FDG that includes vascular and extravascular FDG should be negligible when compared to the phosphorylated FDG. This assumption can also be violated in FDG non-avid tumors where the vascular concentration and/or intracellular non-phosphorylated FDG are increased and the standard imaging time wouldn't be appropriate. In post-therapy conditions, there is also a chance to find an elevated background activity that impacts the SUV uptake profile taken over time [26].

From the above described points, one should be very careful in using the SUV in assessing response to treatment or using the SUV as a surrogate biomarker in clinical trials. The assumption that SUV is correlated with the metabolic rate of glycolysis (MRglu) and thus can be used as surrogate biomarker specially in clinical trials requires validation studies as some new drugs modify the FDG differential uptake due to, for example, increased inflammatory processes in other areas away from the tumor site(s) [27]. In some situations, it has been reported that up to 40 % of FDG uptake occurs in non-tumor tissue in post-therapeutic evaluation [34].

Dual or multiple time point SUV measurement is an intermediate approach between static-based acquisitions and dynamic imaging. It considers the tumor uptake in timely spaced points instead of recording tumor uptake over a certain acquisition period while static because it doesn't look at tracer kinetics during data acquisition. It provides a good means for characterizing a given pathology whether inflammatory (or benign lesion) versus malignant lesions as the former generally shows a pattern of constant or tracer washout, while the malignant tissue often has a persistent or even accumulating uptake pattern (see Fig. 13.4).

Dual time point can serve to improve test sensitivity by improving lesion contrast and test specificity by excluding patients with abnormal or suspected findings. Its utility has been

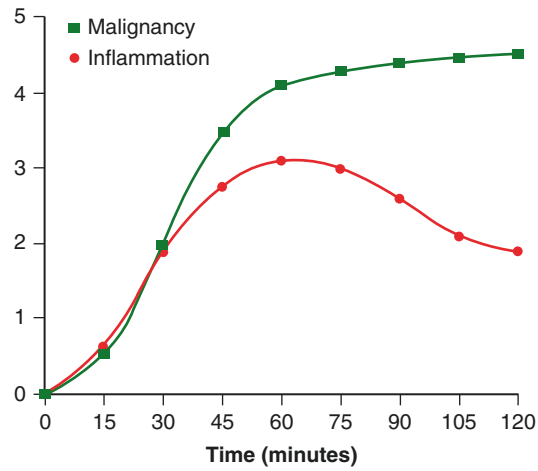

Fig. 13.4 General pattern of F18-FDG uptake in inflammatory and malignant lesions. Inflammatory cells exhibit a sort of transient retention and tracer washout, while cancer cells show a continuous tracer uptake over time (From Hess et al. [13] with permission from Springer Science + Business Media)

demonstrated in a number of malignancies including bone, head and neck, lung, breast, and colorectal cancers and infection or inflammatory disorders [35–38]. However, further efforts need to be exercised along with elaborate guidelines emphasizing the specifics of dual or multiple time points in routine clinical practice [39].

13.3 Standardized Uptake Value (SUV)

SUV is the most commonly used quantitative index in clinical PET imaging. SUV formula is very simple and this form is widely acceptable.

$$\mathrm{SUV} = \frac{\text{Activity Concentration}\left(\text{Voxel or VOI}\right)}{\text{Normalized injected Activity}_{(\text{bw, lbm, or bsa})}}$$

Activity concentration is a quantity derived from a region of interest or voxel taken at a certain single region where the metabolic activity is of considerable clinical value. It can be kBq/ml or μCi/ml or any other equivalent unit.

Normalized injected activity is the administered PET tracer (i.e., injected dose) normalized to patient body weight (BW), body surface area (BSA), or lean body mass (LBM), and decay corrected to the PET acquisition start time. Note that the injected activity (e.g., MBq or mCi) should have the same unit like the one measured from the image 2D ROI, voxel or volume of interest (VOI).

Advantages of SUV are more than onefold. It is easy to calculate, available, and implemented as a built-in tool in viewing or processing workstations of all modern PET/CT scanners. It doesn't also require arterial blood sampling like other methods that rely on dynamic imaging and kinetic modeling as outlined earlier. It can principally be calculated at any single time point after tracer administration. There are several approaches devised to look for what is the most appropriate or representative voxel or group of voxels that accurately and reliably express metabolic activity within a given pathology. Therefore, there are a number of SUV variants that have been proposed in practice and will be discussed later.

Lesion contouring methods are also broad and range from very simple manual delineation to very sophisticated high-order automatic lesion segmentation. There are, however, some variables that need to be highlighted when attempts are made to work on PET data such as image noise, spatial resolution, image filtering, voxel size, degree of heterogeneity in the tumor, and uptake gradient within and outside the tumor relative to the background level [40]. Methods that can model or account for these variables while able to provide accurate and reproducible lesion segmentation can be the most preferable one for clinical adoption and standardization.

Substantial efforts have been carried out to address the problem of manual delineation that is prone to inter-subject and intra-subject variability. Several methods were developed for lesion segmentation task with different statistical or mathematical principles that may include thresholding; edge detection; watersheds; region growing; classifiers; clustering; gradient-based, fuzzy C-means or fuzzy locally adaptive Bayesian, Markov random field models; artificial neutral networks; deformable models; atlas-based methods; and others [41, 42]. Some studies were also conducted to address inherent differences and highlight the relative accuracies of those approaches [43]. However, there is no single optimal solution or consensus acceptable for all clinical problems in terms of accuracy, precision, and efficiency. This is particularly important in multicenter oncology studies where uniform delineation methods are required [44].

Investigators recognize that there is a substantial growing interest in applying fully automatic approaches that are clinically more feasible on efficiency and user-input levels [41]. Image segmentation in research could vary significantly based on the intended application and the adopted method together with the textural or morphological appearance of the oncologic lesions. Therefore, producing a benchmark database for validation and comparison of methods will be very beneficial for PET imaging detection tasks and image processing applications [41].

13.3.1 Drawbacks of SUV

Although the SUV has several quantitative and clinical implications, it has some potential drawbacks. It is simply a temporal and spatial oversimplification of the metabolic and biochemical process in question and doesn't provide a detailed description of tracer kinetics within different tissue compartments [28, 45]. The injected tracer undergoes a number of biochemical interactions that are not accounted for using SUV measurements and through which it may be converted from one chemical species to another or from vascular space to interstitial space or vice versa. Meanwhile, the SUV picks up only the total signal coming from the area of interest where all or some of these processes are taking place [46]. The biodistribution of tracer in a given lesion might include delivery, uptake, retention, and clearance, and these processes can't be separated by a single SUV metric. It is also impossible to separate the various components that contribute to the total signal such as specific binding, nonspecific binding, and free tracer in tissue [27].

Another quantitative shortcoming of SUV comes when using different radiotracers of tumor uptake that is not significantly different from healthy tissues. This situation stimulated researchers to look for alternative quantitative measures that potentially able to discriminate between pathologic lesion kinetics and other type of non-pathologic processes as demonstrated in 3′-[18 F]fluoro-3′-deoxythymidine (18 F-FLT) PET studies [11, 21].

13.3.2 SUV Variants

Quantitative PET and SUV metric has several levels of measurements based on the complexity of computation and the employed analytical methods [40]. The most commonly used SUV metrics are SUV_{mean}, SUV_{max}, and SUV_{peak}. The former is defined using the abovementioned formula for SUV calculations where the numerator is taken as the mean FDG or PET tracer concentration within the region or volume of interest. Measurements of SUV_{max} consider the maximal pixel concentration within the selected lesion. The SUV_{mean} is operator dependant and underestimates the true value especially in small lesions due to partial volume effect. On the other side, SUV_{max} is sensitive to noise as it increases positive bias as noise increases and a subject of debate in response to treatment monitoring [47, 48]. It has also some wrong implications and less representation in heterogenous tumor mass as more than SUV_{max} may exist within the same volume.

One study reported that the variability of SUV_{max} that can be attributed to image noise accounts for half of the overall variability [47]. They also reported that percentage change in $SUV_{max} < 30\,\%$ is still within the uncertainty of repeated measurement, and a positive bias of SUV_{max} can be as high as 30 % for short acquisition time (high noise level), evaluated as 1 min per bed position [47]. SUV_{mean} is much more variable due to operator-dependent factors including size and shape of mask delineation and location within or around a lesion, as well as the presence of tumor heterogeneity and variable level of background 18 F-FDG activity.

SUV_{peak} is the average SUV within a small, fixed-size region of interest (ROI peak) centered on a high-uptake part of the tumor. PET Response Criteria in Solid Tumors (PERCISTs) recommend SUV_{peak} taken for the lean body mass (i.e., SUL) as an index for tumor response [49]. It has several technical definitions as what are the most relevant ROI shape, size, and dimension. The shape can be square or cuboidal of side length of 7–15 mm. In terms of ROI geometries, it can be cylindrical, spherical, or even circular in diameters ranging from 9 to 17 mm [50]. For a given lesion, there might be more than one SUV_{peak}.

In a recent work, a number of 24 SUV_{peak} were used to look for the most appropriate variant in quantification of different tumor response using FLT as biomarker. ROI size was the most influential factor in SUV_{peak} variation when compared to ROI shape or location. In addition and generally, the intra-tumor SUV_{peak} tended to decrease, but its variation tended to increase as the size of ROI_{peak} increased [50]. Therefore, the SUV_{peak}

ROI candidate should be optimally chosen based on well-defined specific criterion in favor of accurate assessment of patient response for individual tumor. One report revealed that SUV_{peak} was the most robust method when using varying reconstruction methods, especially in small lesions when compared to SUV_{mean} and SUV_{max} [51]. In the same report, the latter two showed an increased variability in small lesions <5 ml, while SUV_{peak} remained more stable.

A robust and reliable estimate of SUV should be carried out based on standardized protocol and long-term observation on patient outcome. SUV measures are still "surrogate" biomarker and the accurate determinant, and reference gold standard is patient survival-based treatment response strategy [52]. In most cases, a number of lesion samples are taken to be quantified with less interest to cover all lesions and their metabolic volume or global metabolic activity leading to a relative sampling and assessment error based on the particular region selected. Nevertheless, a growing interest is currently being taken toward evaluating patients based on overall disease burden as follows in the next section.

13.4 Total Disease Burden

Total lesion glycolysis (TLG) is another metric that is used in quantifying total tumor burden. It is simply calculated by multiplying the SUV_{mean} by the lesion volume. This is for a single lesion, but when considering the whole-body tumor burden, then the values of all lesions TLG are summed up. Total metabolic tumor volume (TMTV) on the other hand reflects the total volume of all lesions within the whole body. These measures look at the overall or gross metabolic activity of cancer cells and eventually could be a potential measure of disease status and better candidates for monitoring response to treatment in comparison to uptake measures such as SUV and its variants [53–55].

It was first proposed in patients with Alzheimer to assess disease burden in an age-matched comparison along with partial volume correction [56]. The MR segmented brain structures were multiplied with the mean cerebral glycolytic activity, and end results showed that partial volume-corrected metabolic rates per unit weight of the brain were not significantly different in these cohorts, but that total brain metabolism was significantly lower in patients with Alzheimer. In addition, their efficacy and predictive power in correlation with recurrence-free survival or overall survival have then been investigated in the field of oncology. In cardiology, combining the FDG PET data and CT morphologic imaging of the chest covering the aortic region was proposed in calculating the atherosclerotic burden for each segment of the aorta by multiplying SUV with wall volume [57]. The arterial wall volume was calculated with the help of the CT contrast data delineating the inner and outer area of the aortic segment that appeared on each axial CT slice then subtracting to get the net volume.

In small-cell lung cancer, high TMTV and TLG were associated with poor survival outcomes, and both were reported to be significant independent prognostic factor, whereas SV_{mean} and SUV_{max} were poor measures and showed nonstatistical significance in survival [58]. This was true especially in patients with limited disease rather than extended disease. However, finding a proper and reliable but may be combined prognostic indices could help physicians in taking risk-adapted therapeutic decision and better follow-up treatment strategy. For instance, SUV_{max} and MTV measured on pretreatment ^{18}F-FDG PET/CT in patients with oropharyngeal squamous cell carcinoma have shown to be independent variables in predicting clinical outcomes such as overall survival and disease-free survival [59].

In the context of head and neck cancer in response to chemoradiotherapy, multivariate analysis showed that high MTV (defined as tumor volume with SUV over 2.5) >25.0 mL and high TLG >144.8 g remained as independent significant predictors of incomplete response compared with low MTV and low TLG, respectively. However, predictive efficacy of pretreatment F18-FDG PET/CT varies with different primary sites and chosen parameters. Local response of laryngohypopharyngeal cancer was highly predictable by PET-/CT-based volume measurements [60].

Abgral et al. showed that the retention index (measured as percentage variation of SUV_{max}) and MTV measured for a cohort of head and neck squamous cell carcinoma patients using dual-phase (early-delay) technique were independently correlated with recurrence-free survival [61]. Global disease assessment will likely have great importance for improved pretreatment planning, patient selection for clinical trials, patient stratification, prediction of treatment response, and response assessment. Nevertheless, it was pointed out that the use of a whole-body metric involving TLG could be highly dependent on the severity of partial volume effect, and ignoring this pitfall in small lesions can greatly underestimate the total TLG compromising its potential prognostic value. However, this needs to be evaluated more thoroughly on an individual tumor basis [62].

Combining metabolic information and structural changes from PET and CT, respectively, was also an approach taken to monitor disease response to treatment. While a reduction in tumor volume using multi-detector row CT during chemotherapy for esophageal cancer was found a good predictor of histopathologic response [63], Larson et al. combined anatomic and functional information and monitoring changes using TLG derived from multiplying the tumor volume on CT with the FDG uptake on PET [64].

It should be noted that the new era of molecular-anatomical imaging has witnessed an emergence and advances not only from image co-registration and extracting invaluable diagnostic information but also on the way the data are quantified. Similarly, combining the powerful multiparametric concept in patient diagnosis to interrogate characteristic information of tumor biology within individual patients, despite expensive and technically demanding, can provide a wealth of information that guide physician to more accurate diagnosis and proper treatment.

13.5 Factors Affecting Quantitative Measurements

The quantitative approach implemented in SUV measurements has several sources of error and may lead to great under- or overestimation of the net results. It is not only related to biological factors or physiological conditions but also associated with quite large number of methodological and technical variables [65–67]. There are also some points that need to be addressed that influence SUV during patient preparation and radioactivity injection. Infiltrated or extravasated radioactivity during patient injection serves to underestimate the injected dose described in the SUV formula and hence compromise the SUV measurements [68].

Physical and technical or instrumental factors are also important variables and extend to include image acquisition and data reconstruction, uptake time, count density, reconstruction algorithm, examination time, scanner cross calibration with dose calibrator, and other corrections that include data normalization, dead time, random corrections, scatter and attenuation correction, and partial volume effect (PVE) (details can be found in Chap. 15). Reconstruction algorithm and selection of reconstruction parameters play an important role in the speed and rate of convergence and also to the final spatial resolution of the reconstructed image and might result in increased partial volume effects by making SUV more dependent on surrounding activity distributions [39, 51]. Other factors such as size, shape, and location of ROI/VOI used together with patient weight normalization factor are interplaying to determine the accuracy and reproducibility of SUV. In addition, application of contrast agents and the presence of metallic artifacts in CT images overestimate the attenuation factors and cause a significant elevation of SUV [69]. Patient stress and uncomfortable long waiting or exposure to cold conditions can cause increased uptake in muscle and brown fat affecting SUV measurements [70, 71].

Motion artifact is also one of the major issues in thoracic and abdominal PET imaging due to the blurring effect caused by organ motion during data acquisition. This is particularly important as it can reduce signal-to-noise ratio compromising delineation of lesion borders and corrupting SUV measurements together with less confidence in image interpretation. Several and extensive research works have been carried out to address

this potential artifact and rectify the results of the SUV measurements. This topic was discussed in details in Chap. 16. Consequently, SUV should be carefully interpreted in body regions where motion exists, and thus special emphasis should be placed on longitudinal and follow-up studies [72].

13.5.1 Biological Factors

Accumulation and uptake of FDG within cells and tissues vary considerably, and a better understanding of the time activity profile of the tracer in a region of interest has important implications in data quantification. In the definition of SUV, the tracer concentration is the only variable for a given patient, and injected dose and hence an appropriate time point must be carefully selected to reflect clinically relevant information. This is also particularly important if the tracer accumulation and clearance occur at a relatively fast rate.

A number of studies have been conducted to look at the F18-FDG concentration over time to understand its kinetic parameters and biodistribution profile over body organs. This can potentially provide a baseline information to be used as guidelines for multiple point imaging sessions, using particular regions as reference for other pathologic lesions, or in delayed imaging protocol [73]. While FDG is taking up avidly by tumor cells of high glycolytic activity, its uptake value is less in some other types of tumor cells such as well-differentiated prostate adenocarcinoma and renal cell carcinoma [74, 75]. Furthermore, in poorly differentiated hepatocellular tumors, the degree of FDG uptake is relatively high when compared to well-differentiated tumors. An increased level of background activity can also be seen as concentration of dephosphorylating enzymatic activity (i.e., phosphatases) increases leading to FDG un-trapping and reuptake by normal liver cells. On the therapeutic level, high uptake by infiltrating immune cells can mask the decreased uptake by the dying tumor cells [76]. All the above scenarios have a confounding influence on the quantitative accuracy of PET data and should be placed into proper technical and clinical perspectives.

13.5.2 Blood Glucose Level

As mentioned earlier, the FDG molecule is taken avidly by tumor cells of high glycolytic activity. This interferes with the endogenous glucose to the extent that it may suppress the FDG uptake in the tumor or target cells especially at increased levels of blood glucose levels (e.g., diabetes). However, this was shown to have little effect in inflammatory cells [77]. FDG is a glucose analogue and competes with the plasma glucose through the transmembrane transporters (GLUTs) and intracellular enzymatic activity to enter into the cellular domain. Therefore, increased levels of blood glucose, as in hyperglycemia, play an important role in altering the relative uptake of FDG within different healthy tissues and unhealthy tumor cells. It can significantly reduce the retention of FDG in tumor cells underestimating the SUV measurements. Because of these shortcomings, guidelines have some recommendations of glucose levels for those referred for FDG PET scanning. The European Association of Nuclear Medicine (EANM) recommends that scanning be avoided above 11.1 mmol/L (about 200 mg/dL as an upper threshold limit), and for research the recommended upper plasma glucose levels may range between 7 and 8.3 mmol/L (126 and 150 mg/dL). Similarly, the Society of Nuclear Medicine and Molecular Imaging (SNMMI) recommends rescheduling the patient if the blood glucose level is greater than 150–200 mg/dL [78].

The use of insulin intervention to reduce glucose to normal levels has some characteristics that need to be understood. Insulin regulates glucose uptake into cells by recruiting membrane vesicles containing the GLUT glucose transporters from the interior of cells to the cell surface, where it allows glucose to enter cells by facultative diffusion. Increased levels of insulin in the blood therefore play a molecular role in eliciting the translocation of the GLUT protein transporter, and this phenomenon is significantly apparent in skeletal and cardiac muscles as well as adipose tissues [79].

While some recent optimized protocols for intravenous injection of insulin in diabetic patients were shown to lessen or avoid any

abnormal FDG distribution, there are some other reports that show insulin may lead to unacceptable distribution of 25% of diabetic cancer patients manifested by increased muscle uptake and decreased liver uptake [80]. It appears that insulin injection has some critical precautions that need to be placed into proper perspectives. The method of injection, the dose of insulin, the time between injection and imaging procedure, and the degree of hyperglycemia versus patient tolerance and response all seems to play a relative role in proper management of diabetic cancer patients [81].

In this context, it is important to mention that some drugs do alter the FDG uptake and significant change in SUV measurements can be observed. It has been shown that metformin, for example, significantly increases F18-FDG uptake in the colon and, to a lesser extent, in the small intestine, but lesion quantification might need further evaluation [82]. Stopping metformin has therefore been recommended so that lesion obliteration can be prevented [83]. For a review, see [84].

Attempts made to correct the SUV measurements for blood glucose level were reported to increase variability in test-retest studies when evaluating reproducibility in cancer-free population [85]. In obese patients, the fat contribution to the body composition is relatively large, and the FDG uptake is significantly low. This factor plays a role to overestimate the SUV measurements. This phenomenon is mitigated by using lean body mass or body surface area in SUV calculations [86, 87].

13.6 Response to Therapy

Evaluating patients after or during treatment of cancer represents one of the major challenges that physicians encounter in patient management. PET imaging continues to be a valuable tool to assess and manage cancer patients. A notable advantage of using FDG PET/CT in response monitoring is that metabolic changes often precede anatomical alterations [88]. Furthermore, newly developed targeted therapies may not even result in tumor shrinkage despite having a beneficial effect on patient outcome. FDG PET/CT has also been shown to have the potential to change in diagnosis and/or staging and/or treatment plan in more than one-third of patients with suspected or known malignant disease [89]. In addition, it has been demonstrated that it can detect therapeutic changes that permit physicians to revise or modify treatment protocol at early stages of therapeutic regimen. This has several implications in patient prognosis and survival rates.

The lack of metabolic response on FDG PET indicates primary resistance to the drug and may help identify patients who would benefit from another therapy, while re-emergence of metabolic activity within tumor sites following a period of therapeutic response indicates secondary resistance to the drug [90]. The importance of quantitative PET lies in inter-scan evaluation by providing valuable information about treatment efficacy as well as serving as objective measure of the clinical outcome. FDG uptake during treatment is different from uptake after treatment completion, and hence quantification comes into play [88]. It is not only F18-FDG which is used in drug evaluation and assessment of response to therapy, but also there are some other tracers such as F18-FLT that has been utilized in looking at proliferative capacity of the tumor cells. It has some early response capabilities in treatment monitoring and insensitivity to inflammatory lesions especially after radiotherapy and hence better characterization than FDG in this respect [91].

Some malignancies such as lymphoma can be qualitatively assessed for treatment response, whereas other tumors with less response success rate need a proper quantitative evaluation versus a particular therapy line. This is important to address partial metabolic response versus stable response or disease with further metabolic progression. Another valuable feature is obtained when successive measurements of treatment response would provide more insight into downstream outcomes such as survival [92].

A number of different treatment response criteria have been conducted to provide an objective and standardized assessment of therapy outcome and patient monitoring. Traditionally, the

anatomically based tumor response criteria used were World Health Organization (WHO) and Response Evaluation Criteria in Solid Tumors (RECIST 1.0 and RECIST 1.1) which was introduced by the National Cancer Institute (NCI) [93–95]. The former defines the response as a decrease in the product of two perpendicular diameters of the tumor by 50 %, while RECIST defines partial response as a 30 % decrease in the sum of the diameters of target lesions [95].

In 1981, the WHO first published tumor response criteria, mainly for the use in trials where tumor response was the primary endpoint [96]. The criteria introduced the concept of an overall assessment of tumor burden by summing the products of the two longest perpendicular diameters of the measurable lesions and determined response to therapy by evaluation of change from baseline while on treatment. It is based on 2D lesion measurements, no specific requirements on the number of lesions or the smallest measurable lesion size, and therefore tends to be more subjective and time consuming.

On the other hand, key features of the original RECIST included definitions of minimum size of measurable lesions, instructions on how many lesions to follow (up to ten, a maximum five per organ site), and the use of one-dimensional rather than bidimensional measures for overall evaluation of tumor burden. These criteria have subsequently been widely adopted by several academic and nonacademic institutions as well as industry for trials where the primary endpoints are objective response or progression. There was also an interest from regulatory authorities in accepting RECIST as an appropriate guideline for these assessments [94].

There are two common criteria proposed when using metabolic imaging to evaluate tumor treatment response, namely, the European Organization for Research and Treatment of Cancer (EORTC) and PET Response Criteria in Solid Tumors (PERCISTs), and both have quite different approaches in lesion selection, ROI definition, body habitus normalization (body surface area versus lean body mass), and objective rank of disease status that includes progression or regression [49, 97]. Patients are then classified into different response categories based on the relative change in SUV. These categories include complete metabolic response, partial metabolic response, stable metabolic disease, and progressive metabolic disease.

The EORTC criteria were first published in 1999 and are based on baseline-chosen, lesion-specific regions of interest (ROIs) that are followed on each subsequent scan. The chosen lesions should be the most FDG avid. For SUV calculations, EORTC recommends that SUV should be normalized to body surface area [97]. However, the number of lesions to be measured and minimum measurable metabolic lesion was not specified leading to an increased inter-reader variability.

PERCIST was published in 2009, and some of the above shortcomings were circumvented such as determination of number of lesions, the minimum measurable lesion activity and background level, and the features that must exist in comparing between two scanning procedures [49]. This can improve interobserver variability and provide more reproducible data results. The target lesion is defined as the hottest single tumor lesion (SUL) of "maximal 1.2-cm diameter volume ROI in tumor" or SUL peak. PERCIST only evaluates the SUL peak of the hottest tumor. This is a possible limitation of the approach, and further work is warranted to determine how many lesions are needed for assessment [49].

This region is also selected on the basis of cancer stem cell theory regarded as an indicator of the patient's disease status at the given time point and no need to be located in the same lesion at every instance of evaluation. Conditions applied are such that the SUL peak is at least 1.5-fold greater than liver SUL mean + 2 SDs (in 3-cm spherical ROI in normal right lobe of the liver). If the liver is abnormal, primary tumor should have uptake greater than 2.0 x SUL mean of blood pool in 1-cm diameter ROI in descending thoracic aorta extended over 2-cm *z*-axis [49].

EORTC criteria was the first to provide a classification scheme based on patient treatment response: progressive or stable metabolic disease and partial or complete metabolic response that could be compared to traditional clinical trial

endpoints such as overall survival. Its limitation might be ascribed to that fact that estimation parameters are outlined more as guidelines with options rather than clear definitions. This implies that the observer defines what the ROI size is, whether maximum or mean values should be chosen, how many and which target lesions should be registered, whether the SUVs should be summed or response should be calculated per tumor, and whether there should be a minimum SUV limit that a tumor should exceed in order to qualify as a target lesion [98]. Nevertheless, the EORTC criteria cover quantification of both metabolism and size of the tumor burden, whereas in PERCIST, disease status is determined by the most metabolically active portion of the tumor region.

13.7 Tumor Texture Analysis

Tumor heterogeneity is one of characteristics that can explain the underlying interplaying molecular and genetic factors for a given malignancy and possibly a given stage of disease development. At the time of clinical diagnosis, the majority of human tumors display remarkable heterogeneity in many morphological and physiological features, such as expression of cell surface receptors, and proliferative and angiogenic potential. This heterogeneity might be attributed substantially to morphological and epigenetic plasticity, but there is also strong evidence for the coexistence of genetically divergent tumor cell clones within tumors [99]. It is not generally easy to address this issue by just observing the different color or gray levels during image interpretation, and more objective descriptor can be a surrogate tool providing numerical evidence of tumor heterogeneity.

The process of identification, characterization, understanding, and possibly treatment of tumor heterogeneity is key challenges in oncology and can be an important aid in designing effective cancer therapeutics and monitoring strategies [100]. PET imaging is a promising candidate for determination of tumor heterogeneity within a given tumor mass due to its inherent molecular targeting and capabilities of image quantitation. Other methods have also been reported and of relative strength and weaknesses such as MRI, CT, ultrasonography, and also the use of pathological specimens in lesion characterization [101].

A standard image acquisition, reconstruction, and segmentation protocols are not only prerequisites for uniform data analysis among patients but also for other potential tasks such as establishing a criterion for tumor response assessment as well as in drug development process and clinical trials. Standards are needed to ensure that prospective studies that incorporate textural features are properly designed to measure true effects that may impact clinical outcomes as demonstrated by some investigators [102]. They also found complex trends in variability as a function of textural feature, lesion size, patient size, and reconstruction parameters. The sensitivity of PET textural features to normal stochastic image variation and imaging parameters was found large and is feature dependent.

To investigate the utility of texture analysis in real practice, several studies have been designed to address its clinical value in a number of malignancies. In patients presented with esophageal cancer and treated with combined radiochemotherapy, receiver-operating characteristic (ROC) curve analysis showed that tumor textural analysis was able to identify nonresponder, partial-responder, and complete-responder patients with higher sensitivity (76–92 %) than any SUV measurement providing a stratification mechanism of esophageal carcinoma patients in the context of therapy-response prediction [103].

Pyka et al. and others demonstrated that evidences are growing to indicate that tumor heterogeneity as described by FDG PET texture is associated with response to radiation therapy in non-small cell lung cancer [104]. The results may be helpful into identifying patients who might profit from an intensified treatment regime. In another study from the same group, determination of tumor heterogeneity in pre-therapeutic 18 F-fluoroethyl-L-tyrosine (FET)-PET using textural features was beneficial for the subgrading of high-grade glioma as well as prediction of tumor progression and patient survival. It also showed improved performance compared to

standard parameters such as tumor-background ratio and tumor volume [105]. Those two studies need further verification in a prospective patient cohort before being incorporated into routine clinical practice [104, 105].

Another report has shown that each subtype of non-small cell lung cancer, namely, adenocarcinoma and squamous cell carcinoma, has different metabolic heterogeneity supporting the use of textural parameters in FDG PET as an imaging biomarker [106]. There were 15 texture features that had significant different values between the two different tumor subtypes, and there was no high correlation between SUV_{max} and texture parameters ($|r| \leq 0.62$). Cheng et al. reported that uniformity extracted from the normalized gray-level co-occurrence matrix represents an independent prognostic predictor in patients with advanced T-stage oropharyngeal squamous cell carcinoma [107].

As described earlier, MTV is one of the potential prognostic indices, and correlation with tumor heterogeneity could provide complementary information in the same context. Volume and heterogeneity were found independent prognostic factors ($P = 0.0053$ and 0.0093, respectively) along with stage ($P = 0.002$) in non-small cell lung cancer, but in the esophageal tumors, volume and heterogeneity had less complementary value because of smaller overall volumes [108].

Conclusion

Image quantitation in PET examinations is one of the features that place PET in a unique position in morphological and molecular imaging matrix. Static imaging and dynamic imaging are the two common mode of data acquisition that can be used to derive the required sort of information. The former is the conventional type that used routinely in whole-body PET/CT during clinical practice, whereas dynamic imaging is limited to research activities but able to address "absolute" physiologic information of tracer pharmacokinetics. Due to technical limitation of current designs of PET systems, whole-body dynamic imaging can't be realized, but some trials are being done to overcome such limitation that could make it feasible in the clinic using modified acquisition protocols.

It has become evident that SUV measurements and its intrinsic characteristics of normalization to body weight, lean body mass, or surface body area could have an important implication on the accuracy and reproducibility of tracer quantitation. SUV measurements have several sources of error that could substantially impact its reliability, and thus careful measures need to be undertaken for successful adoption in the clinic.

Quantitative parameters derived from PET imaging data have valuable but differential diagnostic and predictive power in patient prognosis. Several challenges are facing nuclear medicine practitioners to standardize image acquisition, reconstruction, and data analysis so that any interinstitutional variability and systematic errors can be eliminated. This would help in correlating values among different clinics, building up large-scale database and providing more statistical power in data analysis. Now there are many quantitative measures that can be used in patient stratification, prognosis, and predicting tumor response to therapy; however, a universal guidance or general consensus from international societies should be in place to support and optimize the efforts toward finding the best approach for each malignancy.

References

1. Warburg O. On the origin of cancer cells. Science. 1956;123:309–14.
2. Warburg O, Posener K, Negelein E. Über den Stoffwechsel der Carcinomzelle. Biochem Z. 1924; 152:309–44.
3. Vander Heiden MG, Cantley LC, Thompson CB. Understanding the Warburg effect: the metabolic requirements of cell proliferation. Science. 2009; 324:1029–33.
4. Pauwels EK, Ribeiro MJ, Stoot JH, et al. FDG accumulation and tumor biology. Nucl Med Biol. 1998;25:317–22.
5. Hricak H. Oncologic imaging: a guiding hand of personalized cancer care. Radiology. 2011;259:633–40.
6. Vriens D, Visser EP, de Geus-Oei LF, Oyen WJ. Methodological considerations in quantification of

oncological FDG PET studies. Eur J Nucl Med Mol Imaging. 2009;37:1408–25.
7. Bentourkia M. Tracer kinetic modeling: methodology and applications. In: Khalil MM, editor. Basic sciences of nuclear medicine. Berlin/Heidelberg: Springer; 2011.
8. Kjell E. Tracer kinetic modeling: basics and concepts. In: Khalil MM, editor. Basic sciences of nuclear medicine. Berlin/Heidelberg: Springer; 2011.
9. Kostakoglu L, Gallamini A. Interim 18F-FDG PET in Hodgkin lymphoma: would PET-adapted clinical trials lead to a paradigm shift? J Nucl Med. 2013;54:1082–93.
10. Cistaro A, Quartuccio N, Mojtahedi A, et al. Prediction of 2 years-survival in patients with stage I and II non-small cell lung cancer utilizing (18) F-FDG PET/CT SUV quantification. Radiol Oncol. 2013;47:219–23.
11. Tomasi G, Turkheimer F, Aboagye E. Importance of quantification for the analysis of PET data in oncology: review of current methods and trends for the future. Mol Imaging Biol. 2011;14:131–46.
12. Boellaard R. Standards for PET image acquisition and quantitative data analysis. J Nucl Med. 2009;50 Suppl 1:11S–20.
13. Hess S, Blomberg B, Rakheja R, et al. A brief overview of novel approaches to FDG PET imaging and quantification. Clini Transl Imag. 2014;2:187–98.
14. Gholami S, Salavati A, Houshmand S, Werner TJ, Alavi A. Assessment of atherosclerosis in large vessel walls: a comprehensive review of FDG-PET/CT image acquisition protocols and methods for uptake quantification. J Nucl Cardiol. 2015;22:468–79.
15. von Schulthess GK, Steinert HC, Hany TF. Integrated PET/CT: current applications and future directions. Radiology. 2006;238:405–22.
16. Antoch G, Freudenberg LS, Egelhof T, et al. Focal tracer uptake: a potential artifact in contrast-enhanced dual-modality PET/CT scans. J Nucl Med. 2002;43:1339–42.
17. Brechtel K, Klein M, Vogel M, et al. Optimized contrast-enhanced CT protocols for diagnostic whole-body 18F-FDG PET/CT: technical aspects of single-phase versus multiphase CT imaging. J Nucl Med. 2006;47:470–6.
18. Varnas K, Varrone A, Farde L. Modeling of PET data in CNS drug discovery and development. J Pharmacokinet Pharmacodyn. 2013;40:267–79.
19. Klein R, Beanlands RS, deKemp RA. Quantification of myocardial blood flow and flow reserve: technical aspects. J Nucl Cardiol. 2010;17:555–70.
20. Dimitrakopoulou-Strauss A, Pan L, Strauss LG. Parametric imaging: a promising approach for the evaluation of dynamic PET-18F-FDG studies – the DKFZ experience. Hell J Nucl Med. 2010;13: 18–22.
21. Muzi M, O'Sullivan F, Mankoff DA, et al. Quantitative assessment of dynamic PET imaging data in cancer imaging. Magn Reson Imaging. 2012; 30:1203–15.
22. Jones T, Rabiner EA. The development, past achievements, and future directions of brain PET. J Cereb Blood Flow Metab. 2012;32:1426–54.
23. Watabe H, Ikoma Y, Kimura Y, Naganawa M, Shidahara M. PET kinetic analysis – compartmental model. Ann Nucl Med. 2006;20:583–8.
24. Karakatsanis NA, Lodge MA, Tahari AK, et al. Dynamic whole-body PET parametric imaging: I. Concept, acquisition protocol optimization and clinical application. Phys Med Biol. 2013;58:7391–418.
25. Graham MM, Peterson LM, Hayward RM. Comparison of simplified quantitative analyses of FDG uptake. Nucl Med Biol. 2000;27:647–55.
26. Kotasidis F, Tsoumpas C, Rahmim A. Advanced kinetic modelling strategies: towards adoption in clinical PET imaging. Clini Trans Imag. 2014;2:219–37.
27. Lammertsma A, Boellaard R. The need for quantitative PET in multicentre studies. Clini Transl Imag. 2014;2:277–80.
28. Hamberg LM, Hunter GJ, Alpert NM, et al. The dose uptake ratio as an index of glucose metabolism: useful parameter or oversimplification? J Nucl Med. 1994;35:1308–12.
29. Boellaard R, Delgado-Bolton R, Oyen WJ, et al. FDG PET/CT: EANM procedure guidelines for tumour imaging: version 2.0. Eur J Nucl Med Mol Imaging. 2015;42:328–54.
30. Boellaard R, O'Doherty MJ, Weber WA, et al. FDG PET and PET/CT: EANM procedure guidelines for tumour PET imaging: version 1.0. Eur J Nucl Med Mol Imaging. 2010;37:181–200.
31. Fukukita H, Suzuki K, Matsumoto K, et al. Japanese guideline for the oncology FDG-PET/CT data acquisition protocol: synopsis of Version 2.0. Ann Nucl Med. 2014;28:693–705.
32. Gupta N, Gill H, Graeber G, et al. Dynamic positron emission tomography with F-18 fluorodeoxyglucose imaging in differentiation of benign from malignant lung/mediastinal lesions. Chest. 1998;114:1105–11.
33. Karakatsanis NA, Lodge MA, Zhou Y, Wahl RL, Rahmim A. Dynamic whole-body PET parametric imaging: II. Task-oriented statistical estimation. Phys Med Biol. 2013;58:7419–45.
34. Kazama T, Faria SC, Varavithya V, et al. FDG PET in the evaluation of treatment for lymphoma: clinical usefulness and pitfalls. Radiographics. 2005;25:191–207.
35. Hustinx R, Smith RJ, Benard F, et al. Dual time point fluorine-18 fluorodeoxyglucose positron emission tomography: a potential method to differentiate malignancy from inflammation and normal tissue in the head and neck. Eur J Nucl Med. 1999;26:1345–8.
36. Sahlmann CO, Siefker U, Lehmann K, Meller J. Dual time point 2-[18F]fluoro-2′-deoxyglucose positron emission tomography in chronic bacterial osteomyelitis. Nucl Med Commun. 2004;25: 819–23.
37. Tian R, Su M, Tian Y, et al. Dual-time point PET/CT with F-18 FDG for the differentiation of malignant and benign bone lesions. Skeletal Radiol. 2009;38: 451–8.

38. Shimizu K, Okita R, Saisho S, et al. Clinical significance of dual-time-point 18F-FDG PET imaging in resectable non-small cell lung cancer. Ann Nucl Med. 2015;29:854–60.
39. Houshmand S, Salavati A, Hess S, et al. An update on novel quantitative techniques in the context of evolving whole-body PET imaging. PET Clini. 2015;10:45–58.
40. Carlier T, Bailly C. State-of-the-art and recent advances in quantification for therapeutic follow-up in oncology using PET. Front Med (Lausanne). 2015;2:18.
41. Foster B, Bagci U, Mansoor A, Xu Z, Mollura DJ. A review on segmentation of positron emission tomography images. Comput Biol Med. 2014;50:76–96.
42. Zaidi H, El Naqa I. PET-guided delineation of radiation therapy treatment volumes: a survey of image segmentation techniques. Eur J Nucl Med Mol Imaging. 2010;37:2165–87.
43. Tylski P, Stute S, Grotus N, et al. Comparative assessment of methods for estimating tumor volume and standardized uptake value in (18)F-FDG PET. J Nucl Med. 2010;51:268–76.
44. Boellaard R, Oyen WJ, Hoekstra CJ, et al. The Netherlands protocol for standardisation and quantification of FDG whole body PET studies in multicentre trials. Eur J Nucl Med Mol Imaging. 2008;35:2320–33.
45. Keyes Jr JW. SUV: standard uptake or silly useless value? J Nucl Med. 1995;36:1836–9.
46. Huang SC. Anatomy of SUV. Standardized uptake value. Nucl Med Biol. 2000;27:643–6.
47. Lodge MA, Chaudhry MA, Wahl RL. Noise considerations for PET quantification using maximum and peak standardized uptake value. J Nucl Med. 2012;53:1041–7.
48. Boellaard R, Krak NC, Hoekstra OS, Lammertsma AA. Effects of noise, image resolution, and ROI definition on the accuracy of standard uptake values: a simulation study. J Nucl Med. 2004;45:1519–27.
49. Wahl RL, Jacene H, Kasamon Y, Lodge MA. From RECIST to PERCIST: evolving considerations for PET response criteria in solid tumors. J Nucl Med. 2009;50 Suppl 1:122S–50.
50. Vanderhoek M, Perlman SB, Jeraj R. Impact of the definition of peak standardized uptake value on quantification of treatment response. J Nucl Med. 2012;53:4–11.
51. Brendle C, Kupferschlager J, Nikolaou K, et al. Is the standard uptake value (SUV) appropriate for quantification in clinical PET imaging? – variability induced by different SUV measurements and varying reconstruction methods. Eur J Radiol. 2014;84:158–62.
52. Weber WA. Assessing tumor response to therapy. J Nucl Med. 2009;50 Suppl 1:1S–0.
53. Manohar K, Mittal BR, Bhattacharya A, Malhotra P, Varma S. Prognostic value of quantitative parameters derived on initial staging 18F-fluorodeoxyglucose positron emission tomography/computed tomography in patients with high-grade non-Hodgkin's lymphoma. Nucl Med Commun. 2012;33:974–81.
54. Chung HH, Kwon HW, Kang KW, et al. Prognostic value of preoperative metabolic tumor volume and total lesion glycolysis in patients with epithelial ovarian cancer. Ann Surg Oncol. 2011;19:1966–72.
55. Liao S, Penney BC, Wroblewski K, et al. Prognostic value of metabolic tumor burden on 18F-FDG PET in nonsurgical patients with non-small cell lung cancer. Eur J Nucl Med Mol Imaging. 2012;39:27–38.
56. Alavi A, Newberg AB, Souder E, Berlin JA. Quantitative analysis of PET and MRI data in normal aging and Alzheimer's disease: atrophy weighted total brain metabolism and absolute whole brain metabolism as reliable discriminators. J Nucl Med. 1993;34:1681–7.
57. Bural GG, Torigian DA, Chamroonrat W, et al. Quantitative assessment of the atherosclerotic burden of the aorta by combined FDG-PET and CT image analysis: a new concept. Nucl Med Biol. 2006;33:1037–43.
58. Park SB, Choi JY, Moon SH, et al. Prognostic value of volumetric metabolic parameters measured by [18F] fluorodeoxyglucose-positron emission tomography/computed tomography in patients with small cell lung cancer. Cancer Imaging. 2014;14:2.
59. Kim JW, Oh JS, Roh JL, et al. Prognostic significance of standardized uptake value and metabolic tumour volume on (1)(8)F-FDG PET/CT in oropharyngeal squamous cell carcinoma. Eur J Nucl Med Mol Imaging. 2015;42:1353–61.
60. Hanamoto A, Tatsumi M, Takenaka Y, et al. Volumetric PET/CT parameters predict local response of head and neck squamous cell carcinoma to chemoradiotherapy. Cancer Med. 2014;3:1368–76.
61. Abgral R, Valette G, Robin P, et al. Prognostic evaluation of percentage variation of metabolic tumor burden calculated by dual-phase FDG PET-CT imaging in patients with head and neck cancer. Head Neck. 2016;38 Suppl 1:E600–6.
62. Hatt M, Le Pogam A, Visvikis D, Pradier O, Cheze Le Rest C. Impact of partial-volume effect correction on the predictive and prognostic value of baseline 18F-FDG PET images in esophageal cancer. J Nucl Med. 2012;53:12–20.
63. Beer AJ, Wieder HA, Lordick F, et al. Adenocarcinomas of esophagogastric junction: multi-detector row CT to evaluate early response to neoadjuvant chemotherapy. Radiology. 2006;239:472–80.
64. Larson SM, Erdi Y, Akhurst T, et al. Tumor treatment response based on visual and quantitative changes in global tumor glycolysis using PET-FDG imaging. The visual response score and the change in total lesion glycolysis. Clini Positron Imag. 1999;2:159–71.
65. Cook GJ, Wegner EA, Fogelman I. Pitfalls and artifacts in 18FDG PET and PET/CT oncologic imaging. Semin Nucl Med. 2004;34:122–33.
66. Gorospe L, Raman S, Echeveste J, et al. Whole-body PET/CT: spectrum of physiological variants, artifacts

and interpretative pitfalls in cancer patients. Nucl Med Commun. 2005;26:671–87.
67. Mawlawi O, Pan T, Macapinlac HA. PET/CT imaging techniques, considerations, and artifacts. J Thorac Imaging. 2006;21:99–110.
68. Silva-Rodriguez J, Aguiar P, Sanchez M, et al. Correction for FDG PET dose extravasations: Monte Carlo validation and quantitative evaluation of patient studies. Med Phys. 2014;41:052502.
69. Ahmadian A, Ay MR, Bidgoli JH, Sarkar S, Zaidi H. Correction of oral contrast artifacts in CT-based attenuation correction of PET images using an automated segmentation algorithm. Eur J Nucl Med Mol Imaging. 2008;35:1812–23.
70. Hao R, Yuan L, Zhang N, Li C, Yang J. Brown adipose tissue: distribution and influencing factors on FDG PET/CT scan. J Pediatr Endocrinol Metab. 2012;25:233–7.
71. Pace L, Nicolai E, D'Amico D, et al. Determinants of physiologic 18F-FDG uptake in brown adipose tissue in sequential PET/CT examinations. Mol Imaging Biol. 2010;13:1029–35.
72. Nehmeh SA, Erdi YE. Respiratory motion in positron emission tomography/computed tomography: a review. Semin Nucl Med. 2008;38:167–76.
73. Cheng G, Alavi A, Lim E, et al. Dynamic changes of FDG uptake and clearance in normal tissues. Mol Imaging Biol. 2013;15:345–52.
74. Delgado Bolton RC, Mucientes Rasilla J, Perez Castejon MJ, Carreras Delgado JL. Positron emission tomography (PET) and PET-CT in renal, bladder and prostate cancer: update. Actas Urol Esp. 2009;33:11–23.
75. Schoder H, Larson SM. Positron emission tomography for prostate, bladder, and renal cancer. Semin Nucl Med. 2004;34:274–92.
76. Merchant S, Witney T, Aboagye E. Imaging as a pharmacodynamic and response biomarker in cancer. Clini Trans Imag. 2014;2:13–31.
77. Zhao S, Kuge Y, Tsukamoto E, et al. Fluorodeoxyglucose uptake and glucose transporter expression in experimental inflammatory lesions and malignant tumours: effects of insulin and glucose loading. Nucl Med Commun. 2002;23:545–50.
78. Delbeke D, Coleman RE, Guiberteau MJ, et al. Procedure guideline for tumor imaging with 18F-FDG PET/CT 1.0. J Nucl Med. 2006;47:885–95.
79. Young LH, Coven DL, Russell 3rd RR. Cellular and molecular regulation of cardiac glucose transport. J Nucl Cardiol. 2000;7:267–76.
80. Roy FN, Beaulieu S, Boucher L, Bourdeau I, Cohade C. Impact of intravenous insulin on 18F-FDG PET in diabetic cancer patients. J Nucl Med. 2009;50: 178–83.
81. Martin J, Saleem N. 18F-FDG PET-CT scanning and diabetic patients: what to do? Nucl Med Commun. 2014;35:1197–203.
82. Gontier E, Fourme E, Wartski M, et al. High and typical 18F-FDG bowel uptake in patients treated with metformin. Eur J Nucl Med Mol Imaging. 2008;35:95–9.
83. Ozulker T, Ozulker F, Mert M, Ozpacaci T. Clearance of the high intestinal (18)F-FDG uptake associated with metformin after stopping the drug. Eur J Nucl Med Mol Imaging. 2010;37:1011–7.
84. Surasi DS, Bhambhvani P, Baldwin JA, Almodovar SE, O'Malley JP. (1)(8)F-FDG PET and PET/CT patient preparation: a review of the literature. J Nucl Med Technol. 2014;42:5–13.
85. Paquet N, Albert A, Foidart J, Hustinx R. Within-patient variability of (18)F-FDG: standardized uptake values in normal tissues. J Nucl Med. 2004;45:784–8.
86. Kim CK, Gupta NC, Chandramouli B, Alavi A. Standardized uptake values of FDG: body surface area correction is preferable to body weight correction. J Nucl Med. 1994;35:164–7.
87. Kim CK, Gupta NC. Dependency of standardized uptake values of fluorine-18 fluorodeoxyglucose on body size: comparison of body surface area correction and lean body mass correction. Nucl Med Commun. 1996;17:890–4.
88. Allen-Auerbach M, Weber WA. Measuring response with FDG-PET: methodological aspects. Oncologist. 2009;14:369–77.
89. Hoilund-Carlsen PF, Gerke O, Vilstrup MH, et al. PET/CT without capacity limitations: a Danish experience from a European perspective. Eur Radiol. 2011;21:1277–85.
90. Van den Abbeele AD. The lessons of GIST – PET and PET/CT: a new paradigm for imaging. Oncologist. 2008;13 Suppl 2:8–13.
91. Bollineni VR, Kramer GM, Jansma EP, Liu Y, Oyen WJ. A systematic review on [F]FLT-PET uptake as a measure of treatment response in cancer patients. Eur J Cancer. 2016;55:81–97.
92. Doot RK, McDonald ES, Mankoff DA. Role of PET quantitation in the monitoring of cancer response to treatment: review of approaches and human clinical trials. Clini Transl Imag. 2014;2:295–303.
93. World, Health, Organization. WHO handbook of reporting results of cancer treatment. Geneva: World Health Organization; 1979.
94. Therasse P, Arbuck SG, Eisenhauer EA, et al. New guidelines to evaluate the response to treatment in solid tumors. European Organization for Research and Treatment of Cancer, National Cancer Institute of the United States, National Cancer Institute of Canada. J Natl Cancer Inst. 2000;92:205–16.
95. Eisenhauer EA, Therasse P, Bogaerts J, et al. New response evaluation criteria in solid tumours: revised RECIST guideline (version 1.1). Eur J Cancer. 2009; 45:228–47.
96. Miller AB, Hoogstraten B, Staquet M, Winkler A. Reporting results of cancer treatment. Cancer. 1981;47:207–14.
97. Young H, Baum R, Cremerius U, et al. Measurement of clinical and subclinical tumour response using [18F]-fluorodeoxyglucose and positron emission

tomography: review and 1999 EORTC recommendations. European Organization for Research and Treatment of Cancer (EORTC) PET Study Group. Eur J Cancer. 1999;35:1773–82.
98. Skougaard K, Nielsen D, Jensen BV, Hendel HW. Comparison of EORTC criteria and PERCIST for PET/CT response evaluation of patients with metastatic colorectal cancer treated with irinotecan and cetuximab. J Nucl Med. 2013;54:1026–31.
99. Marusyk A, Polyak K. Tumor heterogeneity: causes and consequences. Biochim Biophys Acta. 1805; 2009:105–17.
100. Buvat I, Orhlac F, Soussan M. Tumor texture analysis in PET: where do we stand? J Nucl Med. 2015;56(11):1642–4.
101. Lubner MG, Stabo N, Lubner SJ, et al. CT textural analysis of hepatic metastatic colorectal cancer: pretreatment tumor heterogeneity correlates with pathology and clinical outcomes. Abdom Imaging. 2015;40:2331–7.
102. Nyflot MJ, Yang F, Byrd D, et al. Quantitative radiomics: impact of stochastic effects on textural feature analysis implies the need for standards. J Med Imag (Bellingham). 2015;2:041002.
103. Tixier F, Le Rest CC, Hatt M, et al. Intratumor heterogeneity characterized by textural features on baseline 18F-FDG PET images predicts response to concomitant radiochemotherapy in esophageal cancer. J Nucl Med. 2011;52:369–78.
104. Pyka T, Bundschuh RA, Andratschke N, et al. Textural features in pre-treatment [F18]-FDG-PET/CT are correlated with risk of local recurrence and disease-specific survival in early stage NSCLC patients receiving primary stereotactic radiation therapy. Radiat Oncol. 2015;10:100.
105. Pyka T, Gempt J, Hiob D, et al. Textural analysis of pre-therapeutic [18F]-FET-PET and its correlation with tumor grade and patient survival in high-grade gliomas. Eur J Nucl Med Mol Imaging. 2016;43:133–41.
106. Ha S, Choi H, Cheon GJ, et al. Autoclustering of non-small cell lung carcinoma subtypes on (18) F-FDG PET using texture analysis: a preliminary result. Nucl Med Mol Imag. 2015;48:278–86.
107. Cheng NM, Fang YH, Chang JT, et al. Textural features of pretreatment 18F-FDG PET/CT images: prognostic significance in patients with advanced T-stage oropharyngeal squamous cell carcinoma. J Nucl Med. 2013;54:1703–9.
108. Hatt M, Majdoub M, Vallieres M, et al. 18F-FDG PET uptake characterization through texture analysis: investigating the complementary nature of heterogeneity and functional tumor volume in a multi-cancer site patient cohort. J Nucl Med. 2015;56: 38–44.